Simple Extraction of Region of Interest in Low-field MRI Brain Images

Rajasvaran Logeswaran

Faculty of Computing and Digital Technology, HELP University, Kuala Lumpur, Malaysia
Loges@ieee.org

Received: 01 December 2025 Revised: 10 January 2026 Accepted: 11 February 2026

Abstract

Low-field Magnetic Resonance Imaging (MRI) is used in the operating room to provide real-time images during sensitive surgeries such as those on the brain. The low resolution nature of these images, along with the presence of artifacts and noise, requires pre-processing to extract the region of interest (ROI) – i.e. the brain. The scheme described in this paper achieves this using an approach with low complexity, preparing the image for segmentation and other image analysis tasks. The first of this three-stage approach employs histogram analysis to identify the image intensity distribution characteristics. It is found that there exist three dominant peaks: background, acquisition artifact, and ROI. Selective histogram thresholding is followed by the second stage where denoising filters are applied. Promising results are reported with bilateral filters. Finally, the images are normalized in terms of size, intensity and orientation, for standardized treatment in subsequent tasks. Both qualitative and quantitative results are presented to validate the performance of proposed algorithms.

***Keywords*-**Medical imaging; image denoising; image normalization; image pre-processing; low-field magnetic resonance imaging

1. Introduction

Medical images are produced from various imaging modalities such as Computed Tomography (CT), Positron Emission Tomography (PET), Magnetic Resonance Imaging (MRI), ultrasound and X-Ray scans of various body parts, e.g. brain, shoulder, heart, liver, spine etc. MRI is a non-invasive medical imaging technique used to identify and visualize the structure and function of the body, generally producing good quality images. The most commonly used systems are the high-field MRI (5 - 7 Tesla) and conventional MRI (1.5 – 3 Tesla), both of which require dedicated shielded rooms. As such, they are only applicable pre- and post-surgery, but not during the surgery itself. In recent years, advancement in MRI technology using low-field magnetic strength of 0.15 Tesla has been introduced to overcome this problem.

The much simpler magnet setup for low-field MRI offers many advantages: the possibility of using open magnets (minimizes claustrophobia), less static magnetic field exposure to the surrounding area, less costly equipment that is well-suited in the standard operating room (OR) environment, compatible with the electronic equipment and surgical tools, relatively small in size and practical in cramped spaces. They can even be used at the bedside of patients [1]. With this, real-time scans are possible during the surgery where updated images to reflect changes in anatomy after opening the skull can be obtained. Furthermore, in situations where high-field strengths may drown out subtle signal differences, the low-field MRI becomes invaluable to detect these (such as in differentiating cancerous and non-cancerous tissue).

Several previous studies have compared conventional MRI versus low-field MRI, with most indicating no significant differences in diagnostic interpretations between them [2]. They are clinically applicable in operations and even routine checkups. Generally, higher field strength improves the signal-to-noise ratio (SNR). The contrast and resolution increases almost linearly with field strength. The increased field strength also allows faster scanning and lowers the incidence of motion artifacts.

Unfortunately, although using the same underlying technology, the images produced by low-field MRI differs considerably from the conventional and high-field counterparts, in terms of appearance and quality. Thus, most pre-processing techniques used for the latter are not applicable to low-field MRI images [3]. The main shortcoming of low-field MRI is the low-resolution and artifact surrounding the brain region, which complicates visualization as well as leads to false segmentation (especially for automated systems). There have been efforts to create algorithms to produce super-resolution low-field brain MRI [4], but these machine learning approaches tend to be more complex and require high computational resources.

This paper discusses some characteristics of the low-field MRI brain images and possible steps that could be taken in order to improve its quality and extract the region of interest (ROI), namely the brain, with reduced resource requirements and complexity. This could facilitate quick processing on lower-end processors and be applicable during operations.

The structure of this paper is as follows. The next section discusses some background of the pre-processing techniques to be applied. Section 3 details the methodology undertaken in this work. This is followed by the experiments performed and the corresponding results in Section 4, with discussions presented in Section 5. Section 6 draws the conclusions and recommendations of the proposed approach for ROI extraction in low-field MRI brain images.

2. Background

Image processing techniques make it possible to extract meaningful information from medical images. Brain MRI images provide information of brain parts such as white matter (WM), gray matter (GM), cerebrospinal fluid (CSF), ventricles and skull, brain injuries such as bleeding and skull fracture, and diseases affecting the brain such as tumor. Pre-processing is common for operations with images at the lowest level of abstraction where it is also crucial prior to further processing of the medical images. Brain MRI image pre-processing can be performed for several reasons, including the important goal of making them easier to visually examine and interpret. The common pre-processing techniques are image enhancement [5]-[6], image normalization [7]-[8], denoising [9]-[11], resampling and cropping. For computer-aided systems, the images need to be segmented and labeled, to be used meaningfully and may be used to assist medical experts in their diagnosis. Improving the quality of the low-field MRI brain images, especially through visualization suitable to the human visual system, ultimately results in quick analysis, decision making and more flexibility during the surgery.

Histogram analysis has been widely used in medical image processing. Background rejection is one of the common methods based on histogram analysis, where approximately 10% of the maximum gray level is eliminated [12]. However, since the intensity non-uniformity may exist in all directions, usually the normalization procedure will be repeated for all directions. Identifying optimal threshold(s) is always a challenge in MRI due to the wide variance in inter-patient and inter-image intensity distributions.

In recent years, there has been much research into denoising techniques. The well-known Gaussian filter performs well in smooth areas of the image but removes detail. As a consequence, the Gaussian convolution is optimal in flat parts of the image but edges and textures are blurred as well. Median filters sort the neighboring pixels based on their intensities and are able to suppress noise near edges. Anisotropic-diffusion filters motivated by Perona and Malik [8] have been successfully used for denoising while preserving edges. However, these filters may also preserve some of the original noise which is wrongly interpreted as a meaningful structure.

3. Methodology

The ROI extraction from the raw low-field MRI brain images would have to be done in several stages. A three-stage system is proposed in this work. As shown by the flowchart in Fig. 1, the stages areas follows:

- Stage 1: Background Removal– this stage will mainly remove all the unnecessary background surrounding the brain image. In this stage, histogram truncation will be done progressively until the whole image background is removed. The image intensity range is then normalized (typically, stretched between 0-255 on monitors with bit depth of 8 bits per pixel, bpp).

- Stage 2: Denoising - filtering will be applied with the purpose of removing the remaining noise in the brain tissue. However, it is crucial that the denoising techniques applied perform well in the smooth areas of the brain, and at the same time, preserve the edges.
- Stage 3: Standardization / Normalization –this stage will wrap up the pre-processing steps by cropping, rotating and resizing the image, such that the whole image is normalized for subsequent processing.

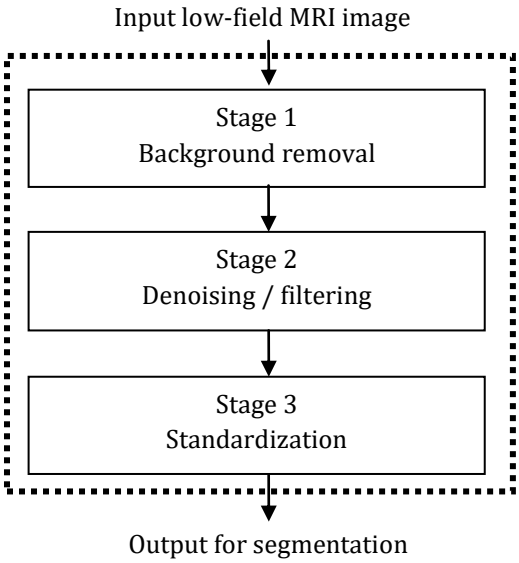

Fig. 1. Proposed system flow for pre-processing technique

3.1Data Collection

As the use of low-field MRI equipment is still not widespread, the number of test images available in this work was limited to a database of 14 patients, each consisting of multiple slice images. Fig. 2 shows a comparison of the visual differences in conventional and low-field MRI images of the brain.

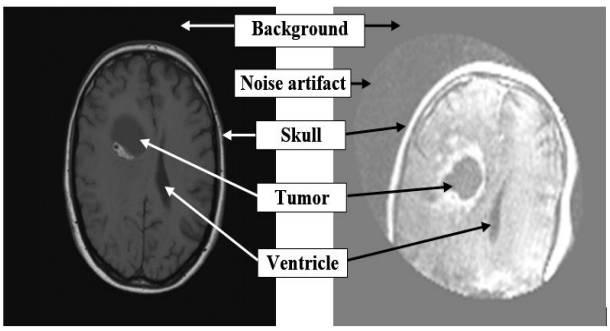

Fig. 2. Comparison between conventional (left) and low-field (right) MRI

Both images were obtained for approximately the same slice (location) of the same patient. However, the quality is noticeably worse in the low-field image. Not only is the noise level increased, but the orientation and coverage of the brain is affected as well due to the small aperture of the low-field MRI equipment. The lower part of the brain is not visible in the low-field image, and a noise artifact is present at the top left. Most image analysis procedures attempt to use only the important information from the image, much of which is obscured in the low-field image. The parts of interest in a typical low-field MRI brain image are labeled in Fig. 2. Any pre-processing techniques undertaken should preserve all the structures in the ROI, which in this case are the labeled areas excluding the artifact and image background.

3.2Histogram Analysis

To identify the low-field MRI image characteristics, each of the 128x128 pixels slice images was analyzed in terms of its intensity histogram. An image having a large number of pixels with very similar brightness values usually presents a histogram with multiple peaks. Often, similar intensities occur in groups or regions, representing similar characteristics in the image, such as a certain anatomical structure, injury or disease. Histogram analysis and manipulation can be used effectively as a pre-processing technique for such grayscale images. The image contrast also provides valuable information for normalization. An image with low-contrast would typically have a narrow histogram, which could be stretched to improve observation clarity.

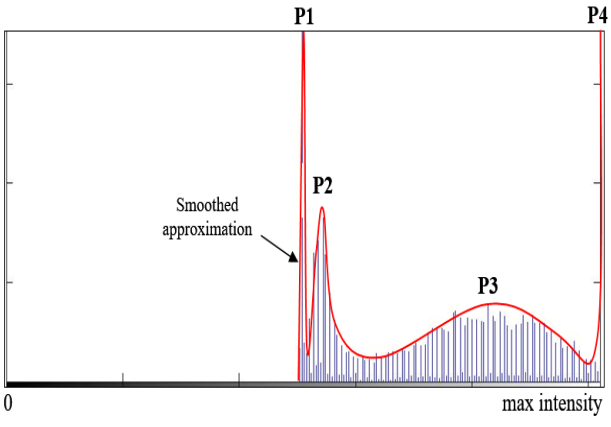

Fig. 3. Histogram analysis of low-field MRI brain

By analyzing the test images, it was found that most of the common low-field MRI brain intensity histograms had three dominant peaks, as shown in Fig. 3. Since peaks and troughs of the histogram are used, as a practical note, local minima and maxima of the frequency distribution would need to be overcome. Function approximation and changing the bin sizes are possible ways of smoothing the histogram. A smoothed approximation of the histogram is shown by the thick line in the figure. Typically, the peaks are as follows:

- The first peak, namely P1, tends to be the highest peak. Being in the very low intensity range, it is expected to be the image background.
- P2, the second peak, beginning after the trough (valley) at the end of the first peak, may contain the pixels in the unwanted noise artifact area.
- Finally, P3, which is situated in the higher intensities, would be expected to cover most of the objects of interest.
- In some images (such as in Fig. 3), a fourth peak (P4) was found at the highest intensity (i.e. 255 in 8 bpp representation). Such images had significant skull areas, and this peak is expected to be the pixels representing the parts of the skull.

To confirm the assumptions above and to gain a better understanding of the images, a step-by-step progressive truncation is undertaken. This process is described in the following sections.

3.3Stage 1 – Background removal

It was observed that the low-field MRI images usually had either a black or grey background with an elliptic artifact around the brain area. Appearing as if part of the head, this artifact could lead to difficulty in interpreting the images, especially to a computer-aided system. Removing the unnecessary background also prevents over-segmentation.

The background has to be removed as it is not part of the brain, thus not part of the ROI. This technique has been used in [12] as one of the pre-processing steps in brain region extraction. It was expected that a distinct peak in the histogram exists for determining the threshold value for the entire image, such that the image could be properly enhanced [13].

Three main steps of processing are to be undertaken in the first stage. These are: background elimination, artifact elimination and finally image normalization, as shown by the flowchart in Fig. 4.

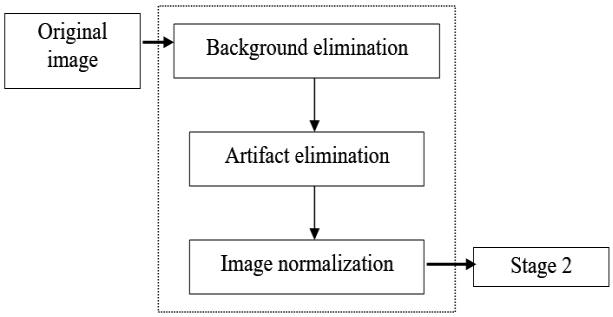

Fig. 4. Flowchart of stage 1 module

The procedure starts off with first completely eliminating the first peak (P1) to remove the black or grey background of the image. This makes the noise artifact visually more obvious and easier to eliminate. By determining the maximum intensity of P2, the intensity range of the elimination technique is chosen using equation(1) below by determining the threshold value (T).

$$T = p(max(P2) - min(P1)) + min(P1) \quad (1)$$

where,
max($P2$) = maximum intensity value at peak P2,
min($P1$) = minimum intensity of the trough after peak P1,
p =the fraction of the slope for each thresholding step (e.g. 1/3).

Next, the input image is thresholded using (2):

$$I_T(i) = \begin{cases} 0 & \text{if } I_O(i) < T \\ I_O(i) & \text{otherwise} \end{cases} \quad (2)$$

where,
$I_T(i)$ = pixel i of the thresholded image,
$I_O(i)$ =pixel i of the original image,
T = the threshold obtained using (1).

Truncating the histogram peaks alone is insufficient since some of the details of the low-field MRI brain are still not seen clearly. Examining the image database further, it was observed that the intensity range of the low-field MRI images were inconsistent, i.e. some in the higher ranges whilst others in the lower ranges. This is typical of MRI images as the

intensity range is not fixed. The visibility of some parts of the brain is improved and made more observable through normalization using (3):

$$\text{Normalized image, } I = \frac{I_T - T}{\max(I_T) - T} \times (2^{Cd} - 1) \quad (3)$$

where,

I_T = thresholded image using threshold T,
$\max(I_T)$ = maximum intensity of I_T,
Cd = color depth (in bpp), e.g. Cd = 8 sets the grayscale intensity range 0-255.

3.4Stage 2 – Denoising

In a wide variety of applications, it is necessary to smooth an image while preserving its edges. The goal of image denoising is to recover the original image from a noisy measurement, satisfying (4).

$$I(i) = I'(i) + n(i) \quad (4)$$

where,

$I(i)$ = the observed value at pixel i,
$I'(i)$= the true value (without noise) of pixel i, and
$n(i)$= the noise perturbation at pixel i.

However, the denoising methods should not alter the original image I'(i). Numerous approaches have been proposed for denoising including the use of Median, Wiener and Gaussian filters. Based on the results deliberated in [14] for denoising of low-field MRI brain images, two denoising methods are taken into consideration in this work, namely anisotropic-diffusion filters and bilateral filters.

Anisotropic-diffusion filters such as the Perona-Malik [8], adjust smoothing strength to the boundaries to reduce the noise while preserving the edges. Consider the anisotropic-diffusion in equation in (5),

$$I' = div\ (c(x,y,t)\ \nabla I) = c\ (x,y,t)\ \Delta I + \nabla c \times \nabla I \quad (5)$$

where,

div = the divergence operator,
∇ and Δ = the gradient and Laplacian operators, respectively.

If $c(x,y,t)$is a constant, equation (5) can be reduced to the isotropic heat diffusion equation in (6),

$$I' = c\Delta I \quad (6)$$

The smoothing will take place separately in each region with no interaction among them, so that the boundaries remain sharp. Edges are enhanced temporarily before slowly blurring them out. There are two main parameters that control the behavior of the smoothing process: the first is the number of iterations which determines how many times the smoothing process is repeated, and the second is the diffusion factor which determines the level of gradient intensity and needs to be adjusted according to the noise level.

Bilateral filters proposed by Tomasi and Manduchi [10], on the other hand, employ a non-iterative and local approach to edge preserving smoothing. The formulation for bilateral filters is summarized as given below:

$$I'(i) = \frac{1}{k(i)} \sum_{\xi \in W_i} I(\xi) \cdot c(\xi, i) \cdot s(I(\xi), I(i)) \quad (7)$$

where,

ξ and i= spatial coordinates,
I = the noisy image,
I' = the filtered image,
W_i = defines the spatial window around pixel i,
$k(i)$ =the normalization constant which assures the weights $c(.).s(.)$ are added up to 1 within W_i.

The functions c and$s$measure the geometric and photometric similarities between neighborhoods, respectively, and are given by (8) and (10), as follows:

$$c(\xi, i) = e^{-\frac{1}{2}\left(\frac{d(\xi,i)}{\sigma_1}\right)^2} \quad (8)$$

where,

$$d(\xi, i) = d(\xi - i) = \|\xi - i\| \quad (9)$$

is the Euclidean distance between pixel ξ and i.

$$s(\xi, i) = e^{-\frac{1}{2}\left(\frac{\delta(I(\xi)I(i))}{\sigma_2}\right)^2} \quad (10)$$

where,

$$\delta\big(I(\xi), I(i)\big) = \delta\big(I(\xi) - I(i)\big) = \|I(\xi) - I(i)\| \quad (11)$$

is a measure of distance between the intensity of pixel ξ and i.

The principal idea of bilateral filters is that it combines both domain and range filtering. The grey levels are combined based on both their geometric closeness and photometric similarity. The degree of

denoising with bilateral filters depends on two values: σ_1 (spatial domain) and σ_2 (intensity domain). However, the time taken depends on the bilateral filter window size, where longer time is needed for a larger window size.

3.5Stage 3 – Standardization

Upon completing Stage 1 and Stage 2, the proposed pre-processing technique is wrapped up by preparing the final image for brain segmentation and further processing (e.g. preliminary diagnosis). Issues such as differing acquisition orientations (shown in the results later) make comparison, analysis and evaluation of the images difficult. An optional overall normalization step, known here as standardization, could help analysis to be conducted more effectively.

The treatment and amount of normalization required may differ on a case by case basis. Some of the expected tasks to be undertaken at this stage include editing to remove rogue background or noise pixels that may have escaped the first two stages, rotation to correct the orientation of the brain image, and cropping of excess parts of the image after the rotation. The editing may be done by going through the image and removing individual or very small clusters of pixels that are likely to be the residues from the earlier stages, for example pixels with high intensity due to impulse-like noise. Pixels outside the skull that are closely related to the background or noise artifacts should be removed as well.

Rotation correction is applied to the images that are tilted to the right or left due to the position of the equipment and patient during the surgery. The images are more easily analyzed in the vertical orientation, as in the conventional MRI images. Clues for rotation correction are derived from the location of known anatomical structures such as the ventricles, through artificially placed markers on the patient, or could be undertaken interactively by the user. Once the orientation is standardized, the image is cropped accordingly, leaving only the brain region. Finally, the resulting image can be resized to a desired frame for easy comparison and analysis.

4. Results

To validate the performance of the proposed algorithm, it was tested on the available database of low-field MRI brain images. The database included patients with various types of brain diseases and injuries such as tumor, bleeding, fracture and abnormalities, in addition to normal brain images. The variety of images allows for better evaluation of the accuracy of experiments conducted. The results obtained at each of the three stages are given below.

4.1Stage 1

The raw images are first evaluated in Stage 1. Fig. 5(a) shows one of the original images used for the experiment, along with its intensity histogram. First and foremost, elimination of P1 is done since it is expected to be the background of the image. Referring to Fig. 5(b), as the first peak is eliminated, the image background surrounding the elliptical area around the brain is removed. This supports the assumption that the first peak consists mostly of the background and the truncation applied eliminates the background accordingly.

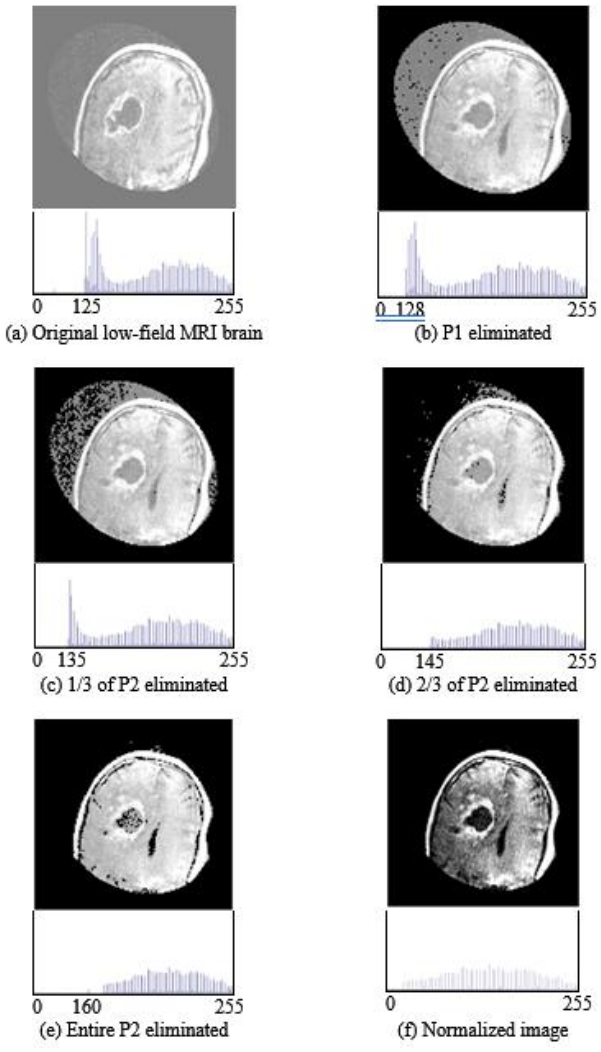

Fig. 5 Step-by-step background removal in Stage 1

To further eliminate the insignificant regions, 1/3 of the second peak (P2) of the histogram is truncated (p = 1/3), as shown in Fig. 5(c). If p is very small (e.g. p = 1/5), the differences in the result is not visually observable, but very large steps (e.g. p = 1/2) should be avoided as significant regions may go missing during this process. From the figure, it is observed that a large amount of the noise artifact managed to be removed, without affecting the ROI. Hence, it is possible to proceed with another 1/3 histogram truncation (i.e. p = 2/3). The result of this is given in Fig. 5(d), showing that most of the distracting noise artifact has been successfully removed. The brain region can be identified clearly as compared to the original image.

Since there are still undesired spots of noise in the image, the whole second peak is then removed. By referring to Fig. 5(e), it is now proven that almost all the visible area of the unwanted region has now been eliminated. Even though some pixels are missing in the tumor region as they had the same intensity value as this threshold, the few missing pixels do not hold any serious consequence on the analysis of the overall image.

To make the image brightness and contrast more uniform, the truncated histogram is stretched so that its intensity range would be in the range from 0 to 255 (it is assumed that an 8 bpp color depth is used in this work). Fig. 5(f) shows the histogram stretched from the 160-255 range to 0-255. A clearer image is produced and hence leads towards better identification of the ROI. The brain folds become more visible and boundaries between tumors inside the brain tissue are enhanced. This eases analysis and reduces the time and cost of processing for the subsequent stages.

4.2Stage 2

Two different denoising filters were tested in this stage, namely anisotropic-diffusion and bilateral. A comparison between the normalized image, and the denoised images using the anisotropic-diffusion and bilateral filters, is shown in Fig. 6.

In Fig. 6(b), although a significant amount of smoothing was applied using the Perona-Malik anisotropic-diffusion filter with 10 iterations and diffusion coefficient of 1 on the normalized image, it still managed to retain the sharp edges.

As for bilateral filter with σ_1 = 100 and σ_2 = 10, the overall shading is preserved, as seen in Fig. 6(c). This is because it is well within the band of the domain filter and almost unaffected by the range filter. Both the techniques managed to sharpen the boundaries between brain tissues and tumor, produced clearer skull separation and made the folds in the brain tissues more visible.

Fig. 6. Denoising techniques applied on normalized image (Stage 2)

As visual evaluation of the results does not shown significant variations, a further comparison of the performance of the denoising filters is done. The signal-to-noise ratio (SNR) is calculated for each brain part in the images as an indication of the image quality. The SNR is equal to the ratio of average signal intensity over the standard deviation of the background noise. Three obviously visible brain parts and one diseased structure, i.e. ventricle, brain tissue, skull and tumor, were selected for the comparison.

The results obtained are given in Table 1. From the results, it is found that bilateral filters have the highest SNR. As such, it was decided that this filter would be selected for the denoising.

Table 1. Signal-to-noise ratio (SNR) for different brain parts

Brain parts	Normalized	Anisotropic-diffusion	Bilateral Filters
Ventricle	140.26	141.84	**149.58**
Tumor	74.96	98.51	**115.02**
Skull	318.37	344.53	**367.31**
Tissue	903.92	907.15	**917.59**

4.3Stage 3

In some MRI brain pre-processing applications, image editing is not an essential step. However, to enhance the result of the ROI extraction to be presented for further analysis, the processed image is further normalized to minimize inter-image variations. The background and residual pixels are removed. Since relative size is useful for analysis and diagnosis, resizing the image to a standard size would be useful for subsequent applications.

Furthermore, it was noticed that some low-field MRI brain images obtained were tilted due to the patient's position during the scanning, and that the tilt angle differed in different sets of images. Image rotation is applied to correct this problem. All the steps taken to synchronize the images allow for the extracted ROI to be presented in a normalized manner that minimizes analysis confusion for the user. As observed in Fig. 7, a clear, vertically oriented ROI is obtained through the proposed methodology.

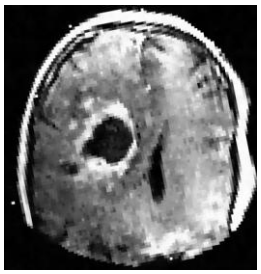

Fig. 7. Final pre-processed image (Stage 3)

4.4Alternative Processing

An alternative approach to histogram truncation discussed in Section 2 is truncation by shifting the original histogram to the left as shown in Fig. 8(a). This approach shifts the histogram to the left and truncates the peaks (e.g. P1). However, although the noise artifact is still present, it appears dimmer and is no longer visually obvious.

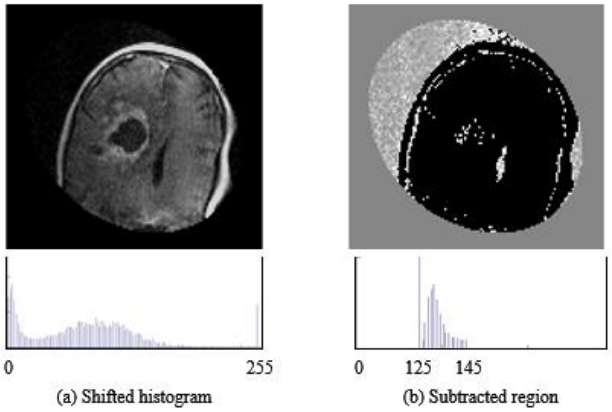

Fig. 8. Additional information for alternative processing

The step-by-step truncating process will hence be more difficult as the resulting effect of the amount of elimination applied is not discernible. Thus, it is not desirable to shift the histogram to the left prior to histogram truncation. Nonetheless, the same final result is obtained by using this technique once the second peak (P2) is removed. For reference, Fig. 8(b) shows the parts of the image that is removed as the whole of P1 and P2 are truncated. Note that the brightness and contrast has been adjusted in order to highlight the removed pixels.

4.5Test results

The results of the various stages show that the proposed methodology is effective in producing a good visual image of the ROI in a low-field MRI brain image. When considering brain surgeries, it is crucial that the significant regions such as tissue, ventricle, tumor, bleeding or skull fracture are highlighted. The extracted ROI results of some of the other test images from patients with different diseases and characteristics are given in Fig. 9. Theseinclude images of normal brain, those with tumor, bleeding and skull fracture, and one taken post-operation. As is observed, the proposed algorithm was able to successfully extract the ROI of the test images with good accuracy.

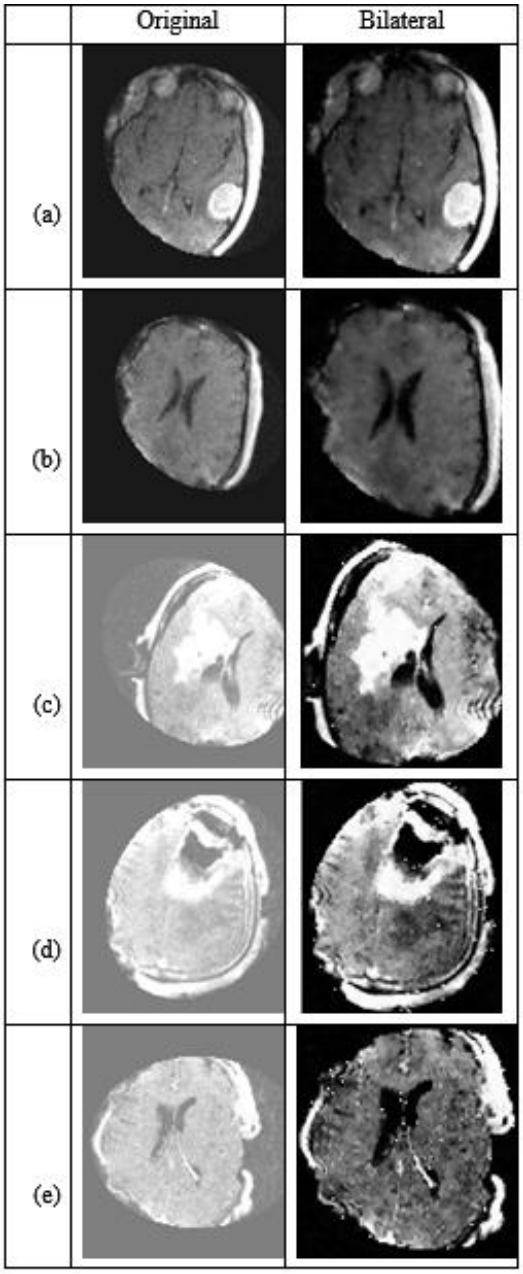

Fig. 9. Results of the ROI extraction on some low-field MRI brain test images

To further justify the steps proposed in the earlier section, five patient's brain scan with different diseases, namely, blood clotting, normal brain, bleeding, post-operation and skull fracture are used to compare the results as shown in Fig. 9. The unnecessary background and artifact have been successfully eliminated from the raw image. Denoising technique applied on the images performed well in smoothing the texture and at the same time, preserved the edges between the high-contrast region such as bleeding or skull and low-contrast region such as ventricle. On the other hand, the first four images had been reoriented, where the brain region was tilted between 0° and 10°.

There are several limitations in this study, in addition to the small patient database. It is difficult to have variety sets of images for low-field MRI brain since only a few medical institutions are using low-field machine as an alternative to conventional MRI. Thus, the comparability between the images is restricted due to this matter. Secondly, diagnosis is being made through visibility by human eyesight. Although, this is what is done in a clinical setting, it may not be the best practical solution in some cases. However, in the experiments conducted, no misclassification was encountered as there were no irregular diseases detected in the database.

5. Discussion

Although the intensity range for each image may differ from each other, the patterns between them are almost similar. Moreover, similar peaks exist in these images, allowing for the proposed algorithm to produce good results even when the brightness and contrast differs between images. Image normalization does not improve only the intensity distribution by making it more similar between images, it also improves the brightness and contrast, thus improving visualization as well.

Denoising may be applied before or after the histogram truncation. However, in this work, it made more sense to undertake the removal of the unrelated areas in the image surrounding the brain first, to minimize their influence on the ROI. Image denoising is helpful in smoothing the image and removing the remaining noise in the image. It has been observed that smoothing the brain tissue and preserving the edges give better results in recognizing the details in the images. However, the greatest challenge in denoising the images is region blending at the edges between brain tissue and tumor or bleeding, as the gradients there can be subtle.

6. Conclusion

Low-field MRI is a technology that can be safely used in operating rooms, at the point-of-care venue or other resource-constrained environments [15]-[16], where the images produced are valuable for guidance and assessment during the diagnosis, surgery and treatment. However, the low signal

strength produces very low resolution images with noise. The small aperture often scans a smaller area than conventional MRI, and analysis can be made difficult by the distracting elliptical noise artifact that could be wrongly assumed to be part of the head when used in scanning the brain. This issue would become more prevalent with the more recent developments, such as the ultra low-field MRI for brain analysis [17].

This study shows that implementation of a pre-processing algorithm to extract the brain ROI in low-field MRI brain images is crucial in order to accurately segment the brain image further. This study developed a step-by-step pre-processing method that leads to ROI extraction in raw low-field MRI brain images. The method proposed in this work integrates histogram analysis, image denoising and image normalization. Given a brain image, histogram analysis is performed to remove the unnecessary background and noise artifact in the image, followed by denoising to smoothen the image and normalizing to standardize the intensity range and orientation of the extracted ROI. Tests conducted on a database of low-field MRI brain images with different characteristics, diseases and injuries confirmed the effectiveness of the technique in producing good visualization results of the brain area. The normalized extracted ROI is expected to benefit the medical specialists in making their diagnosis, as well as enable automated systems to process such images more easily.

Acknowledgement

The author would like to thank the Department of Neurosurgery, Maastricht University Hospital and the Department of Biomedical Engineering, Eindhoven University of Technology (TU/e), for providing the MR images. This project is supported by the Ministry of Science, Technology and Innovation (MOSTI), Malaysia through the Science Fund grant, and conducted in collaboration with researchers N. F. Ishak and W. H. Tan of Multimedia University, Malaysia.

References

[1] V. Mathew, T. R. Lim, A. Nair, A. W. Lin, J. Kosowan, Y. A. Chen, A. Bharatha, and S. Mathur, "Portable Bedside Low-field MRI for Assessment of Ventricular Size", American Journal of Neuroradiology, 2025, doi: 10.3174/ajnr.A8811

[2] T. Magee, M. Shapiro, and D. Williams,"Comparison of high-field-strength versus low-field-strength MRI of the shoulder", American Journal of Roentgenology, 2003, pp 1211 – 1215

[3] N. F. Ishak, M. J. Gangeh, and R. Logeswaran, "A preliminary study of high-field MRI image enhancement techniques applied to low-field MR brain images", 4th International Conference on Biomedical Engineering, vol. 21, 2008, pp. 482 – 486

[4] J. E. Iglesias,R. Schleicher,S. Laguna,B. Billot,P. Schaefer,B. McKaig, J. N. Goldstein,K. N. Sheth,M. S. Rosen, and W. T. Kimberly, "Accurate super-resolution low-field brain MRI", 2022, https://arxiv.org/pdf/2202.03564

[5] M. Garcia, E. Fernandez, M. Grana, and F. J. Torrealdea,"A gradient decent MRI illumination correction algorithm", Computational Intelligence and Bioinspired Systems, vol. 3512, 2005, pp. 913 – 920

[6] L. Gao, J. Jiang, and S. Y. Yang,"Constrained region growing and edge enhancement towards automatic semantic video object segmentation", Advanced Concepts for Intelligent Vision Systems, 2006, pp 323 – 331

[7] Y. L. Liao, N. T. Chiu, C. M. Weng, and Y. N. Sun,"Registration and normalization techniques for assessing brain functional images", Biomedical Engineering Applications, Basis & Communications, vol. 15, no. 3, 2003, pp. 87-94

[8] J. G. Park, T. Jeong, and C. Lee,"Automated brain segmentation algorithm for 3D magnetic resonance brain images", 2nd International Workshop on Soft Computing Applications, 2007, pp. 57 – 61

[9] P. Perona andJ. Malik,"Scale-space and edge detection using anisotropic diffusion", IEEE Transactions on Pattern Analysis and Machine Intelligence, vol. 12, 1990, pp. 629 – 639

[10] C. Tomasi andR. Manduchi, "Bilateral filtering for gray and color images", Proceedings of the IEEE International Conference on Computer Vision, 1998, pp. 839 – 846

[11] A. Buades, B. Coll, and J. M. Morel,"A non-local algorithm for image denoising", Computer Vision and Computer Recognition, vol. 2, 2005, pp. 60 – 65

[12] C. S. Yung, S. H. Ki, M. N. Seung, and W. P. Jong WP,"Threshold estimation for region segmentation of MR image of brain having the partial volume artifact", 5th International Conference on Signal Processing Proceedings, vol. 2, 2000, pp. 1000 – 1009

[13] M. B. Ahmad and T. S. Choi,"Local threshold and Boolean function based edge detection", IEEE Transactions on Consumer Electronics, vol. 45, 1999, pp. 332 – 333

[14] N. F. Ishak, M. J. Gangeh, and R. Logeswaran,"A preliminary study of high-field MRI image enhancement techniques applied to low-field MR brain images", 5th International Conference on Computer Graphics, Imaging and Visualization, 2008, pp. 345 – 349

[15] K. Chetcuti, C. Chilingulo, M.S. Goyal, L. Vidal, N.F. O'Brien, D.G. Postels, K.B. Seydel, and T.E. Taylor, "Implementation of a Low-Field Portable MRI Scanner in a Resource-Constrained Environment: Our Experience in Malawi", American Journal of Neuroradiology, 2022,doi: 10.3174/ajnr.A7494.

[16] T. R. Lim, S. Suthiphosuwan, J. Micieli, R. Vosoughi, R. Schneider, A. W. Lin, Y. A. Chen, A. Muccilli, J. J. Marriott, D. Selchen, S. Mathur, J. Oh, and A. Bharatha, "Low-Field (64 mT) Portable MRI for Rapid Point-of-Care Diagnosis of Dissemination in Space in Patients Presenting with Optic Neuritis", American Journal of Neuroradiology, 2024,doi: 10.3174/ajnr.A8395

[17] P. Hsu, E. Marchetto, D. K. Sodickson, P. M. Johnson, and J. Veraart, "Morphological Brain Analysis Using Ultra Low-Field MRI", Human Brain Mapping, vol. 46, no. 10, 2025, p. e70232, doi: 10.1002/hbm.70232.